International Journal of Solids and Structures 92–93 (2016) 64–75

Contents lists available at ScienceDirect

International Journal of Solids and Structures

journal homepage: www.elsevier.com/locate/ijsolstr

Multiphysics analysis of an asymptotically correct piezoelectric sensor under static and dynamic load

Shreya Banerjee, Sitikantha Roy*

Department of Applied Mechanics, Indian Institute of Technology-Delhi, New Delhi 110016, India

ARTICLE INFO

Article history:
Received 8 December 2015
Revised 14 April 2016
Available online 26 April 2016

Keywords:
Piezoelectric
Variational asymptotic method
Sensor
Recovery

ABSTRACT

This paper presents a versatile platform named Variational Asymptotic Method (VAM), to model and analyze a piezoelectric cantilever sensor under static and dynamic load. Variational asymptotic method is a mathematically rigorous dimentional reduction methodology and has been previously used to model different structures which can be defined by an energy functional having one or more small inherent parameters; but, it has never been explicitly applied to capture the multiphysics behavior of a sensor. Piezoelectric based sensing technology has seen an explosive growth in the last decade with its various applications in different domain, such as energy harvesters, aerospace application, soft robotics, wind turbine, biomechanics, etc. So, an efficient mathematical model is highly required to get a better insight of the multiphysics behavior of an electromechanical structure. The present study highlights the capability of the theory to effectively capture the electromechanical response of a piezo-sensor under any static or dynamic load. The example problems considered in this present study include a single layer piezo-sensor as well as a double layer piezo-sensor bonded with aluminum. For static analysis, we have testified the model under a constant tip load. The discussed method effectively captures the voltage distribution across the thickness of the structure which is one of the fundamental parameter for a sensor model. The response accuracy obtained through variational asymptotic method is very good compared with the 3D simulation response performed in ABAQUS. For dynamic analysis a single layered piezo-sensor has been studied under a tip harmonic force. The structure response is studied for both damped as well as undamped conditions. Displacement and corresponding voltage output for specific excitation frequency which is close to its first natural frequency has been studied. The model efficacy under dynamic load has been validated with the experimental study performed by Ly et al. (2011). The present model has numerous potential applications like in PZT cantilever design for chemo-sensing, disease diagnostic, energy harvesting for self powered electronics, AFM higher harmonic imaging etc. The present theory along with the piezoelectric physics have been implemented in a modified version of VABS II (2004).

1. Introduction

A piezoelectric sensor can be defined as “A device that uses piezoelectric effect, to measure changes in pressure, acceleration, temperature, strain or force by converting them to electrical charge or voltage”. Piezoelectric effect was first discovered by Pierre Curie in the year 1880, and only in the late 1950s piezoelectric effect started to be used for industrial sensing applications. Piezoelectric sensors converts mechanical energy into electrical energy, which can be stored and used to power other devices as well, like self powered electronics (Sodano and Inman, 2005; Ng and Liao, 2005). The reduction in power requirements of small electronics has motivated many researchers to use piezoelectric sensors as alternative power source, which has found various application in remote and wireless sensing technology. Williams and Yates (1996) proposed the three very basic sensing mechanisms, i.e. electromagnetic, piezoelectric and electrostatic. Among these three sources, piezoelectric has proved to be the most prominent one. Chee et al. (2006) has reviewed on the mathematical models that were proposed on piezoelectric transduction. Yang and Lee (1994) showed some of the early works on structures with piezoelectric layers which included a stepped beam model that can predict analytically the natural frequencies and mode shapes at different piezoelectric sensor actuator locations. Similarly, Shen (1994) developed a one dimensional theory for modeling and analysis of a beam with piezoelectric actuators and sensors. Wang and Quek (2002) proposed an Euler beam model with embedded piezoelectric layers and have discussed two ways of connecting the electrodes on the

* Corresponding author. Tel.: +91 8527059228.
E-mail address: sroy@am.iitd.ac.in, sitiroy@gmail.com (S. Roy).

http://dx.doi.org/10.1016/j.ijsolstr.2016.04.025
0020-7683/

surfaces of the piezoelectric layers. A digital regulator was designed and experimentally implemented for a beam containing piezoelectric sensor and actuators by Abreu Gustavo et al. (2003). The procedure as mentioned in the paper for placing the sensors and actuators along the smart structure found to be very effective. Experiments were also performed which demonstrates the effectiveness of the developed controller in reducing the vibration of the fexible beam. A FE-model for static and dynamic analysis of piezoelectric bimorph was discussed by Wang (2004). It combines 2D single layer representation model for mechanical displacement field and layer wise like approximation for the electric potential field. A PVDF bimorph beam and PZT plate were used to verify the present model. Kapuria and Yasin (2010) proposed an efficient FE-model for active vibration control of smart laminated beams integrated with electroded piezoelectric sensors and actuators. Kapuria's model discussed a beam element with two conventional nodes and one electric mode. The directional actuation and sensing using piezoelectric fiber reinforced composite (PFRC) actuators and sensors in active vibration suppression was examined for smart fiber metal laminate plate (Kapuria and Yasin, 2013). Zhou et al. (2005) presented an analytical model of piezoelectric multilayer cantilever as a micro chemical sensor. The voltage output from the model is in millivolt range and can be an appropriate alternative to the conventional laser based position sensitive detection system. There are wide field of application of piezoelectric sensors such as bitmap charge mode force sensor (Kursu et al., 2009), strain sensor based on piezoelectric paint film with its major applications in structural vibration monitoring (Payo and Hale, 2011), MEMS silicon based AC current sensor (Olszewski et al., 2014) and energy harvesters based on bending mode (Ly et al., 2011) and shear mode (Zhoua et al., 2012). A muscle contracting sensing system was presented by Han and Kim (2013) where using piezoelectric probes a resonance based active muscle stiffness sensor was developed to measure stiffness change in muscles. Recently, Buxi et al. (2014) investigated a frequency sensing circuit for measuring low level medical vibrations from ceramic piezoelectric sensor. Kalantarian et al. (2015) developed a necklace based piezoelectric sensor to monitor eating habits which is very crucial for maintaining a healthy lifestyle. Piezoelectric materials are distinguished mainly on the remarkable property to create a conversion interface between two forms of energy, i.e. mechanical and electrical energy. Ajitsaria et al. (2007) and Dalessandro and Rosato (2005), modeled a piezoelectric bender for voltage generation and studied the dynamic response. The modeling of the intelligent (piezoelectric) structures can be categorized in terms of structural configurations (Ali et al., 2004) and also according to the type of modeling. Mathematical modeling is the key element in the design process to understand various interrelated parameters. Any dimensionally reduced structure can be mathematically modeled by three basic approaches. Firstly, Newtonian approach which is based on force and moment balance, secondly asymptotic approach based on the asymptotic expansion of the 3D terms and thirdly variational asymptotic method (VAM) which includes the merits of varitaional approach along with asymptotic approximations of the 3D functional without any ad hoc or previous kinematic assumptions. Variational asymptotic method was first introduced by Berdichevsky (1979). The methodology works with the merits of both variational methods as well as asymptotic methods. One of the essential requirements of VAM based analysis is the existence of the small parameters, and a governing functional, whose extremum leads to the correct solution of the problem. In short, VAM can be termed as a rigorous mathematical tool applicable to any problem governed by an energy functional having one or more small parameter like slenderness for a beam like sensor model which we are trying to analyze here. Yu and Hodges (2004) have discussed how variational asymptotic method (VAM) has a strong mathematical foundation which is able to reproduce numerically the same result for a beam as one obtains from three dimensional elasticity but with less computational cost. VAM was successfully used to model composite beam (Yu, 2002) as well as smart beams with piezoelectric fiber composites (Roy et al., 2007; Neto et al., 2009). Recently a fully coupled rod model was developed by Roy and Yu (2009). Yu et al. (2012) also discusses three updates in the theory for a composite beam model. But the direct piezoelectric effect, i.e. the sensory effect has not yet been analyzed using this theory.

In this present study a sensor has been analyzed as a slender beam model with cantilever boundary condition. The methodology works on by taking advantage of the slenderness of the structure and asymptotically splitting the original 3D problem into a 2D coupled cross-sectional analysis and a 1D beam analysis. The cross-sectional analysis has been implemented using finite element in the computer code VABS, which when combined with 1D beam analysis provide an asymptotically correct 1D constitutive model for smart beams without special assumptions regarding the geometry and the material of the cross-section, distribution of the electric field, the location of the smart materials such as embedded or surface mounted. With the 1D constitutive model and the recovery relations, we can get the full 3D responses of the sensor model. The validation of mathematically rigorous 3D recovery module for a sensor is another key contribution of the present study. Thus variational asymptotic method is a valid methodology which can be used to avoid the difficulties in dealing with the 3D elasticity solution for the same problem. Some standard sensor examples have been studied thoroughly like a cantilever beam with piezoelectric material bonded with aluminium and subjected to external static load as well as a sensor under time varying load, validated with the 3D simulation results obtained from Abaqus/CAE 6.10, Dassault system (2010) and with experimental results (Ly et al., 2011) to prove the accuracy and efficacy of the present theory for piezoelectric sensing. The excellent agreement between the present theory and ABAQUS 3D multiphysics simulation as well as with experimental results demonstrates that one can use this mathematical model to greatly simplify the overall procedure without significant loss in accuracy.

2. Methodology

Fig. 1 projects an overview of the methodology used to develop the mathematical model of sensor. The rectangles represent the analysis and the ellipses represents the bodies of input and output data. The geometry and the material properties of the piezoelectric cantilever beam are the input to the 2D cross-sectional analysis. The 2D cross-sectional analysis is performed by VABS (Variational asymptotic beam sectional analysis) written in FORTRAN 90. Cesnik and Hodges (1997) provides a seminal work in developing VABS. The work done by Hodges (2006) in his book Nonlinear Composite Beam Theory and Yu (2002) in his Ph.d. work, provides the background and theory for VABS. Later Roy (2007) during his Phd work extended the theory for electromechanical structures made up of piezoelectric material. Thus, VABS used for this current work is a modified version of VABS II released in the year 2004 (Yu, 2011) with an addition of piezoelectric physics.

3. Kinematics of the structure

The sensor model in our present study has been analyzed as a slender beam made up of piezoelectric material. So we will try to analyze a beam and its electromechanical behavior. Kinematics deals with the relationship between strains and displacements. The main feature of the sensor model consists of mechanical and electrical fields. The mechanical sub-divison comprises of the 3D strain

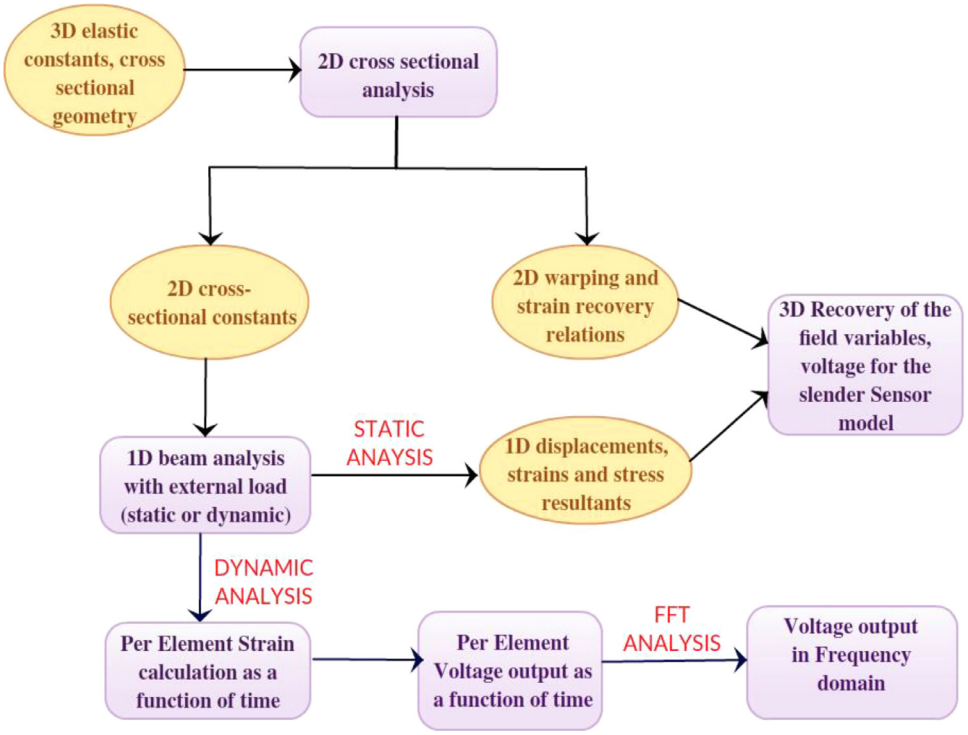

Fig. 1. Flow chart of methodology.

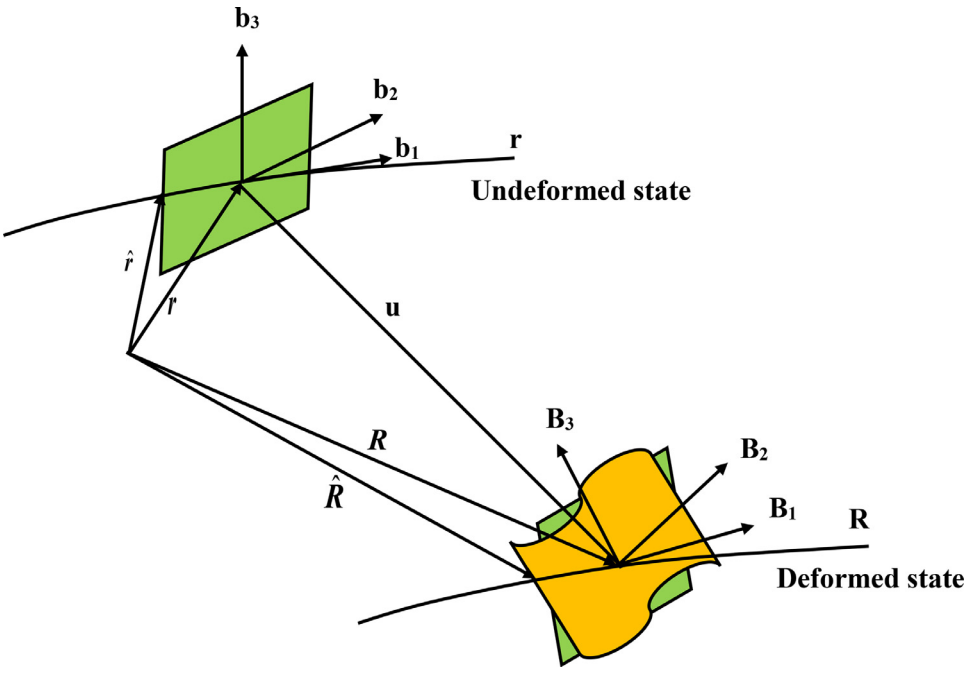

Fig. 2. Schematic of beam deformation.

(Γ_{ij}) related to the 1D strains (ϵ) and in the electrical sub-divison relates the electric field ($\boldsymbol{E}$) to the electric potential (ϕ).

3.1. Mechanical and electrical field

As shown in the Fig. 2, beam is represented by a reference line r measured by x_1, and a typical cross section S with h as its characteristic dimension and described by the curvilinear coordinate system x_α. The cross section can be viewed as a moving 2D domain along the reference line r. An orthonormal triad $\boldsymbol{b}_i$ is introduced at each point along the reference line which is tangent to x_i.

The position vector of any point $\hat{\mathbf{r}}(x_1, x_2, x_3)$ of the undeformed structure can be defined as,

$$\hat{\mathbf{r}}(x_1, x_2, x_3) = \mathbf{r}(x_1) + x_\alpha \mathbf{b}_\alpha \tag{1}$$

where, $\mathbf{r}(x_1)$ is the locus of the points in the reference line. Similarly, the position vector in the deformed state in terms of generalized warping(w_i) is given as,

$$\hat{\mathbf{R}}(x_1, x_2, x_3) = \mathbf{R}(x_1) + x_\alpha \mathbf{B}_\alpha(x_1) + w_i(x_1, x_2, x_3)\mathbf{B}_i(x_1) \tag{2}$$

where $\boldsymbol{B}_i$ is the new triad to define the deformed state and $w_i(x_1, x_2, x_3)$ are the warping functions

The 1D generalized strain measures can be defined as,

$$\gamma_{11}\mathbf{b}_1 = \mathbf{b}_i\mathbf{B}_i \cdot \mathbf{R}' - \mathbf{r}'$$
$$\kappa_i\mathbf{b}_i = \mathbf{b}_i\mathbf{B}_i \cdot \mathbf{K} - \mathbf{k} \tag{3}$$

where $\mathbf{K}$ is the curvature vector of the deformed reference line and $\mathbf{k}$ is the curvature vector of the undeformed reference line, γ_{11} is the extensional strain, κ_1 is the twist and κ_α are the bending curvatures. In all equations, Greek indices varies from 2 to 3 and Roman indices varies from 1 to 3. But complete description of electromechanical structure requires not only mechanical field but also electric field, which is characterized by the electric potential, $\varphi(x_i)$, as

$$\mathbf{E} = -\nabla\varphi = -\frac{\partial\varphi}{\partial x_i}\mathbf{g}^i \tag{4}$$

where, $\mathbf{g}^i$ are the contravarient base vectors.

Using the concept of decomposition of rotation tensor where small local rotations are small, we can express the Jaumann–Biot–Cauchy strains,

$$\Gamma_{ij} = 1/2(F_{ij} + F_{ji}) - \delta_{ij} \tag{5}$$

where δ_{ij} is the Kronecker symbol, and F_{ij} is the mixed-basis component of the deformation gradient tensor such that,

$$F_{ij} = \mathbf{B}_i \cdot G_k g^k \cdot \mathrm{b}_j \tag{6}$$

By combining Eqs. (5) and (6) we get the 3D mechanical strain field in terms of 1D generalized strain measures. For convenience of derivation, we arrange the 1D strains, warping vector and 3D strain vector in matrix notations given as,

$$\epsilon = [\gamma_{11}\kappa_1\kappa_2\kappa_3]^T$$
$$\hat{w} = [w_1 w_2 w_3 \varphi]^T$$
$$\Gamma = [\Gamma_{11} 2\Gamma_{12} 2\Gamma_{13} \Gamma_{22} 2\Gamma_{23} \Gamma_{33} E_1 E_2 E_3]^T \tag{7}$$

From Eqs. (4) and (5), we have the following operator equation for a classical model of a slender beam structure made up of piezoelectric material,

$$\Gamma = \Gamma_h\hat{w} + \Gamma_\epsilon\epsilon \tag{8}$$

with each operator matrices of size 9×4 as referred in Roy et al. (2007). Eq. (8) is of importance since it is now linear in $\hat{w}$, ϵ.

The enthalpy for linear piezoelectric beam is the Legendre transformation of internal energy and can be calculated as,

$$U = \frac{1}{2}\int_0^L \left\langle \Gamma^T \begin{bmatrix} C^E - e^T \\ -e - \varepsilon^\Gamma \end{bmatrix} \Gamma\sqrt{g} \right\rangle dx_1 \equiv \frac{1}{2}\int_0^L \left\langle \Gamma^T C \Gamma \sqrt{g} \right\rangle dx_1 \tag{9}$$

where L denotes the length of the beam, e is the piezoelectric coupling matrix, ε^Γ is the dielectric matrix at constant strain and C^E is the elastic property matrix at constant electric field. The angle brackets signify integration over the cross-sectional plane. Following a similar derivation as done in Roy et al. (2007). The kinetic energy of a beam can be obtained from 3D velocity field as,

$$K = \frac{1}{2}\int_V \rho v^T v dV = K_{1D} + K^* \tag{10}$$

where ρ is the mass density, v the absolute velocity of the generic point in the structure. K_{1D} contains only functions of x_1 and $K*$ contains 3D unknown functions related to the warping functions $w_i(x_1, x_2, x_3)$ and their time derivatives. The order of $K*$ is estimated to be higher than $\mu\epsilon^2$ where μ is the order of the elastic constant, ϵ is the strain and is small as we are working on linear elastic model, h is the size of the cross-section and l the wavelength of the axial deformation. Thus $K*$ can be neglected for the present study.

Similarly we can calculate the virtual work due to the applied loads as,

$$\delta\bar{W} = \delta\bar{W}_{1D} + \delta\bar{W}^* \tag{11}$$

Thus 1D virtual work and the kinetic energy are of same order $\delta\bar{W}_{1D} \sim K_{1D}$.

The elastodynamics of the sensor model can be goverened by the Hamilton's principle as,

$$\int_{t_1}^{t_2} [\delta(K - U) + \overline{\delta W}]dt = 0 \tag{12}$$

For the dynamic problems, Hamilton's principle can be reformulated in terms of 1D displacements and rotations and 3D warping functions as,

$$\int_{t_1}^{t_2} [\delta(K_{1D} + K^* - U) + \delta\bar{W}_{1D} + \delta\bar{W}^*]dt = 0 \tag{13}$$

For static case, the governing function constitutes the potential,

$$\int_{t_1}^{t_2} [\delta U - (\delta\bar{W}_{1D} + \delta\bar{W}^*)]dt = 0 \tag{14}$$

The terms of order $\mu\epsilon^2$ are kept for classical level approximation.

4. Small parameters and order estimation

4.1. Small parameters

The main fundamental behind the present theory lies in dimensionally reducing a structure in such a way so that the computational cost is reduced without much loss in accuracy. This can be achieved by taking advantage of the inherent small parameters that are present in the structure. The small parameters considered in the sensor analysis are:

- Strains: The 3D and the 1D strain field are assumed to be small since we are dealing with geometrically nonlinear but materially linear theory. This means that the structure should always induce strains which are of very small magnitude under any working condition.
- $\frac{h}{l}$ and $\frac{h}{R}$ ratio: Another feature of the present structure is that it should be slender, which means $\frac{h}{l} \ll 1$ and $\frac{h}{R} \ll 1$. Here h is the characteristic size of the cross section, l denotes the characteristic wavelength of axial deformation and R is the characteristic radius of initial curvatures and twist of the beam. Since we are dealing with a sensor model without any initial twist or curvature so $R \to \infty$. For non-prismatic beam, h/R and h/l are assumed to be of the same order and for prismatic beam $h/R = 0$. The existence of these small parameters characterizes a slender structure.

4.2. Order estimation

Order estimation is important to find the relative orders of terms in the strain expression and subsequently in the energy expressions. Since, in the analysis the strain is small, so the order of magnitude of strain is small i.e,

$$\bar{\epsilon} \sim O(\epsilon) \sim O(\Gamma) \ll 1 \tag{15}$$

$\bar{\epsilon}$ is the magnitude of the strain and is the maximum strain the material can withstand. We can also estimate $x_\alpha \sim O(h)$ and $k_i \sim O(\frac{1}{R})$.

From Eqs. (8) and (15) and using the above order estimation we can obtain the relative order magnitudes of other quantities,

$$\gamma_{11} \sim O(\epsilon),\ \kappa_i \sim O\left(\frac{\epsilon}{h}\right) \text{ and } w_i \sim O(h\epsilon) \tag{16}$$

Therefore, we can estimate the order of 3D strain till zeroth order as given in Eq. (8)

$$\left(\Gamma_h \hat{w} + \Gamma_\epsilon \epsilon\right) \sim O(\epsilon) \tag{17}$$

The strain energy density U will be of order $\mu\bar{\epsilon}^2$ where μ is the order of elastic constants. The virtual work and the kinetic energy are of same order as strain energy. The 1D equation of motion as given in Hodges (2006), the following orders of applied forces and moments can be estimated,

$$F_1 \sim O\left(\frac{\mu h \epsilon}{h}\right), \quad Q_1 \sim O(\mu h \epsilon), \quad F_\alpha \sim O\left(\frac{\mu h^2 \epsilon}{h}\right),$$
$$Q_\alpha \sim O(\mu h^2 \epsilon) \tag{18}$$

For low frequency sensor vibration,

$$\frac{h}{c_s \tau} \sim O(h) << 1 \tag{19}$$

where, τ is the scale of change of displacement and warping functions in time and $c_s = \sqrt{\frac{\mu}{\rho}}$ is the characteristic velocity of shear waves (Roy et al., 2007).

5. Dimensional reduction

The dimensional reduction from a 3D formulation to 1D formulation cannot be done exactly. We have to rely on the small parameters as discussed in the previous section. The warping field and the induced potential which are unknown and are discretized within the cross section. The warping field discretized within the elements as,

$$\hat{w}(x_1, x_2, x_3) = S^u(x_2, x_3) V(x_1, t) \tag{20}$$

where S^u is the element shape function and is of $4 \times 4n$ dimension, n being the number of nodes in the element. V refers to the nodal values of the warping and of dimension $4n \times 1$. Total number of degree of freedom in the element is $4n$. The zeroth order strain terms are $\Gamma = \Gamma_h \hat{w} + \Gamma_\epsilon \epsilon$ and of $O(\epsilon)$ as mentioned in Eq. (17). Warping field should not satisfy the equation $\Gamma_h \hat{w} = 0$ to contribute to the zeroth order energy, or mathematically warping functions should be orthogonal to the null space of the operator Γ_h. The solution of the unknown warping can be mathematically given as,

$$\left\langle \hat{w}^T \Psi_1 \right\rangle = 0 \tag{21}$$

where Ψ_1 is the null space matrix of order 4×5.

Eq. (21) results in five constraints on warping such as,

- 3 rigid body translational constraints on warping i.e, $\langle w_1 \rangle = 0$, $\langle w_2 \rangle = 0$ and $\langle w_3 \rangle = 0$.
- The global rotational constraint in the 2–3 planes i.e, $\langle x_2 w_3 - x_3 w_2 \rangle = 0$.
- Constraint on the unknown electric potential as $\langle \phi \rangle = 0$.

To deal with the electric potential at some specific location, the total nodal values of the warp field are divided into two parts such as,

$$V = V_k + V_u \tag{22}$$

here V_k is the known electric potential matrix at specific points (nodes). For sensor model it will comprise of zero volt as we are imposing grounded boundary condition at the interface for the two layer sensor model and at the bottom surface for the single layer sensor model. V_u is the unknown matrix with nodal values of electric potential as zero at the specific points where the electric potential is applied externally. For sensor model the prescribed values of the V_u will be also zero volts.

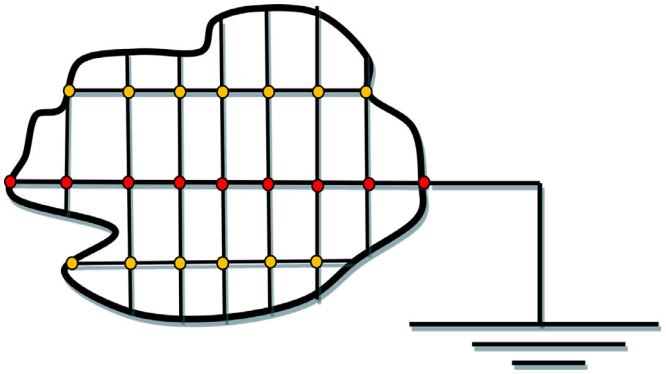

Fig. 3. Meshed cross section.

In the Fig. 3, we can see an arbitary cross section is meshed, the mid nodes which are darkened with red are grounded hence V_{ext} will be allotted zero voltage in the V_k matrix. Thus the V_u and V_k matrices for any p^{th} node on which potential is applied externally is given as,

$$V_u = \begin{bmatrix} \ldots \overbrace{V_{w_1} V_{w_2} V_{w_3} 0}^{p^{th}\text{node}} \ldots \end{bmatrix}^T \text{ and } V_k = \begin{bmatrix} \ldots \overbrace{0\,0\,0\,V_{ext}}^{p^{th}\text{node}} \ldots \end{bmatrix}^T \tag{23}$$

For sensor model in our present study $V_{ext} = 0$ volt for the nodes which are grounded.

For an arbitrary q^{th} node in which the potential is not specified will have,

$$V_u = \begin{bmatrix} \ldots \overbrace{V_{w_1} V_{w_2} V_{w_3} V}^{q^{th}} \ldots \\ \phi \end{bmatrix}^T \text{ and } V_k = \begin{bmatrix} \ldots \overbrace{0\,0\,0\,0}^{q^{th}} \ldots \end{bmatrix}^T \tag{24}$$

These are the point constraints on the electric potential.

6. Constitutive model

From order assessment in the last section we can obtain the leading terms of order $\mu\epsilon^2$ in the variational statement in Eq. (13) to get the zeroth order approximation valid for classical model as,

$$\int_{t_1}^{t_2} [\delta(K_{1D} - \int_0^L U_0 dx_1) + \delta \bar{W}_{1D}] dt = 0 \tag{25}$$

where,

$$U_0 = \frac{1}{2} \langle \Gamma_0^T C \Gamma_0 \rangle \tag{26}$$

and

$$\Gamma_0 = \Gamma_h \hat{w} + \Gamma_\epsilon \epsilon \tag{27}$$

U_0 denotes the zeroth-order approximation of the electromechanical enthalpy functional per unit span of the sensor and obtained through a simplified variational problem,

$$\delta U_0 = 0 \tag{28}$$

over the cross section of the beam sensor and referred as the cross-sectional minimization problem. Substituting Eq. (20) into Eq. (27) along with Eq. (26) we obtain the expression for zeroth order approximation for electromechanical enthalpy as,

$$2U_0 = V^T E V + 2V^T D_{h\epsilon} \epsilon + \epsilon^T D_{\epsilon\epsilon} \epsilon \tag{29}$$

where, $E = \langle [\Gamma_h S^u]^T C [\Gamma_h S^u] \rangle$, $D_{h\epsilon} = \langle [\Gamma_h S^u]^T C [\Gamma_\epsilon] \rangle$ and $D_{\epsilon\epsilon} = \langle [\Gamma_\epsilon]^T C [\Gamma_\epsilon] \rangle$. Solving in the similar way as given in Roy et al. (2007) and applying the constraints as discussed in Eq. (21) we

finally get the zeroth order generalized approximation of the electric enthalpy in discretized form as,

$$2U_0 = \epsilon^T(\hat{V}_0^T D_{h\epsilon} + D_{\epsilon\epsilon})\epsilon + \underline{\epsilon^T(\hat{V}_0^T E V_k + D_{h\epsilon}^T V_\varphi + 2D_{h\epsilon}^T V_k)} \tag{30}$$

In Eq. (30) the underlined term is linear function of ϵ and will be zero for a sensor analysis. Thus with Eq. (30) along with Eq. (25) we get a 1D generalized form suitable for a sensor analysis.We can define the 1D constitutive law by relating 1D generalized resultant forces on the beam cross section with the 1D generalized strains as given by,

$$F = \frac{\partial U_0}{\partial \epsilon} \tag{31}$$

Hence the 1D constitutive model for the classical analysis of a slender sensor model is,

$$\begin{bmatrix} F_1 \\ M_1 \\ M_2 \\ M_3 \end{bmatrix} = S\epsilon = \begin{bmatrix} s_{11}s_{12}s_{13}s_{14} \\ s_{12}s_{22}s_{23}s_{24} \\ s_{13}s_{23}s_{33}s_{34} \\ s_{14}s_{24}s_{34}s_{44} \end{bmatrix} \begin{bmatrix} \gamma_{11} \\ \kappa_1 \\ \kappa_2 \\ \kappa_3 \end{bmatrix} \tag{32}$$

In Eq. (32), S is the stiffness matrix, $[\gamma_{11}\kappa_1\kappa_2\kappa_3]^T$ is the generalized 1D strains which define the deformation of the reference line (γ_{11}: extension, κ_1: twist per unit length, κ_2, κ_3: curvature in 2 and 3 directions) of the beam and F is the conjugate resultant force vector. This 1D analysis generates the strains, which act as an input for the recovery analysis. From recovery analysis we can get the electric potential which is the main parameter to study any type of sensor model.

7. Recovery

7.1. Static recovery

The strain energy of the structure can be written as,

$$U_{1D} = \int_0^L 1/2\epsilon^T F dx_1 \tag{33}$$

Substituting it in Eq. (25) we get a 1D simplified functional to solve for the 1D beam analysis. 1D beam analysis gives the global outlook of the sensor model, including solutions to 1D displacements and 1D generalized strains. To calculate the electric potential we need the recovery relations. By recovery relation we mean expressing the three dimensional displacements, stress and strains in terms of the one dimensional generalized beam quantities, displacements and local cross-sectional coordinates. Mechanical warping and most importantly electric potential is expressed in terms of 1D strains from the recovery relations.

The three dimensional displacement field U_i of the model can be expressed from subtracting Eq. (2) from Eq. (1),

$$\begin{aligned} U_i(x_1, x_2, x_3) = {} & u_i(x_1) + x_\alpha[C_{\alpha i}(x_1) - \delta_{\alpha i}] \\ & + C_{ij}^T(x_1) w_j(x_1, x_2, x_3) \end{aligned} \tag{34}$$

where u_i is the one dimensional beam displacement which is simply the average of the three dimensional displacement variables over the cross-sectional plane. C_{ij} is the components of the direction cosine matrix representing the finite rotation of the cross-sectional frame of the deformed beam ($B_i = C_{ij}b_j$).

The three dimensional strain field can be recovered from the following,

$$\Gamma_0 = \Gamma_h \hat{w} + \Gamma_\epsilon \epsilon \tag{35}$$

From the zeroth order asymptotically correct theory and by minimizing the zeroth order strain energy subjected to constraint, warping function can be obtained in discretized form as (Roy et al., 2007),

$$V_u = V_0\epsilon + V_\phi \tag{36}$$

where, $\hat{w} = S^u V_u \epsilon$, S^u: shape function matrix. Hence substituting Eq. (36) in Eq. (35) we get,

$$\Gamma_0 = \Gamma_h S^u(V_0\epsilon + V_\phi) + \Gamma_\epsilon \epsilon \tag{37}$$

where the three dimensional *generalized strain* field is defined as Γ_0.

7.2. Dynamic recovery

Unlike static case, in the dynamic analysis, 1D strain vector ϵ is a function of space and time,

$$\epsilon(x_1, t) = [B(x_1)]^T\{d(t)\} \tag{38}$$

where B is the strain displacement matrix for a single beam element. For a two noded, constant strain hermitian beam element in planer bending it is expressed as,

$$B^T = \left[H_1'' H_2'' H_3'' H_4''\right] \tag{39}$$

H_1'', H_2'', H_3'' and H_4'' are the second derivative of Hermite interpolation functions and $\{d(t)\}$ is the nodal degrees of freedom, for a single element as a function of time. Once, the 1D strains are calculated from the 1D beam analysis, the voltage over a cross-section is recovered as

$$\phi(x_1, x_2, x_3, t) = [0 \quad 0 \quad 0 \quad 1]\, S^u(x_2, x_3) V_u \epsilon(x_1, t) \tag{40}$$

The output voltage at the electrode surface is calculated as the average potential of the surface nodes which defines the eletoded surface.

7.3. Frequency response analysis

Time domain analysis is always not the best choice especially when it is needed to span a range of frequencies which is otherwise not possible in time domain. Most of the structures under vibration can be characterized by their inherent frequency components. If we excite a system in its natural frequency then in frequency domain analysis we can clearly see the resonance peak corresponding to that natural frequency of excitation. Any signal $x(t)$ which can be represented as,

$$x(t) = \frac{1}{2\pi} \int_{-\infty}^{\infty} X(f) e^{i(2\pi f)t} df \tag{41}$$

where $X(f)$ is the Fourier transform of the time domain signal $x(t)$.

$$X(f) = \int_{-\infty}^{\infty} x(t) e^{-i(2\pi f)t} dt \tag{42}$$

The time signal $x(t)$ is called the inverse Fourier transform of $X(f)$ and also $\int_{-\infty}^{\infty} |x(t)| dx$ should have a finite value. This constraint contains a wide range of signals for a system under dynamic load. Fourier transform involves integral of time varying complex variables which are not easy for calculation. Discrete Fourier transform is an efficient technique to perform such numerical intergration.

Fourier transform is always defined for certain discrete frequency points where the frequency points should be in the range of Nyquist critical frequency i.e.

$$f_e = \frac{1}{2\Delta t} \tag{43}$$

Or else we can say that the sampling period (Δt) should be at least half of the period of signal to sufficiently represent the signal.

Let us assume that there are N sampled values where,

$$x_k = x(t_k), \quad t_k = k\Delta t \text{ and } k = 0, 1, 2.....N-1 \tag{44}$$

Table 1
Material properties of piezo-sensor.

Properties	PZT4	Aluminum
$E_{11} = E_{22}$ (GPa)	81.3	68.9
E_{33} (GPa)	64.5	68.9
G_{12} (GPa)	30.6	27.56
$G_{13} = G_{23}$ (GPa)	25.6	27.56
ν_{12}	0.329	0.25
$\nu_{13} = \nu_{23}$	0.432	0.25
$\varepsilon_{11} = \varepsilon_{22}(\frac{C}{Vm})$	6.761×10^{-9}	10.18×10^{-11}
$\varepsilon_{33}(\frac{C}{Vm})$	5.874×10^{-9}	10.18×10^{-11}
$e_{31} = e_{32}(\frac{C}{m^2})$	−5.2	0
$e_{33}(\frac{C}{m^2})$	15.08	0
$e_{24} = e_{15}$	12.7	0

Table 2
Material property and geometry of piezo-sensor under dynamic load.

Properties	PZT5H
$E_{11} = E_{22}$ (GPa)	60
E_{33} (GPa)	48.16
G_{12} (GPa)	23
$G_{13} = G_{23}$ (GPa)	23.3
ν_{12}	0.2906
$\nu_{13} = \nu_{23}$	0.5099
$\varepsilon_{11} = \varepsilon_{22}(\frac{C}{Vm})$	1.503×10^{-8}
$\varepsilon_{33}(\frac{C}{Vm})$	1.3×10^{-8}
$e_{31} = e_{32}(\frac{C}{m^2})$	23.3
$e_{33}(\frac{C}{m^2})$	−6.5
$e_{24} = e_{15}$	17.0
Length (m)	0.049
Width (m)	0.0038
Thickness (m)	0.0006

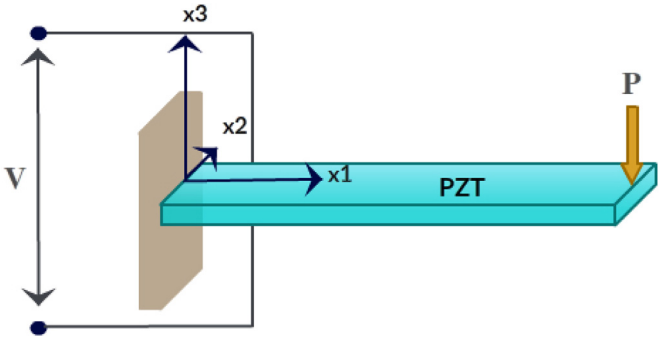

Fig. 4. Single layer piezo-sensor.

Hence the signal can be represented as,

$$X(f_n) = \int_{-\infty}^{\infty} x(t) e^{2\pi i f_n t} dt \sim \sum_{k=0}^{N-1} x_k e^{2\pi i f_n t_k} \Delta t \tag{45}$$

Eq. (45) represents the Discrete Fourier transform and it always has a symmetry property with respect to the input frequency (f_n). Only half of the transform is needed to represent all frequency components.

8. Sensor model validation

In this section, results obtained by using variational asymptotic method to analyze a sensor has been compared with the results obtained from 3D simulation performed in ABAQUS 6.10. ABAQUS is a finite element based generalized tool. VABS which provides the mathematical background of the theory for multiphysics analysis predicts the generalized stiffness for sensor model. It is also capable of generating stiffness along with recovered 3D electrical and mechanical variables for any sensor model with arbitary cross-section, embedded or surface mounted. The model validation starts with static analysis. Examples 8.1 and 8.2 discusses a sensor model under a constant tip load and with cantilever boundary condition. Two different configurations, single layer and double layer sensor model has been studied in Examples 8.1 and 8.2. Example 8.3 highlights a single layer piezoelectric sensor model under a periodic time varying load. In the dynamic analysis the time domain signal has been converted into a frequency domain signal to study the response and corresponding voltage generation for a particular excitation frequency. The material property and the geometry are listed in Tables 1 and 2.

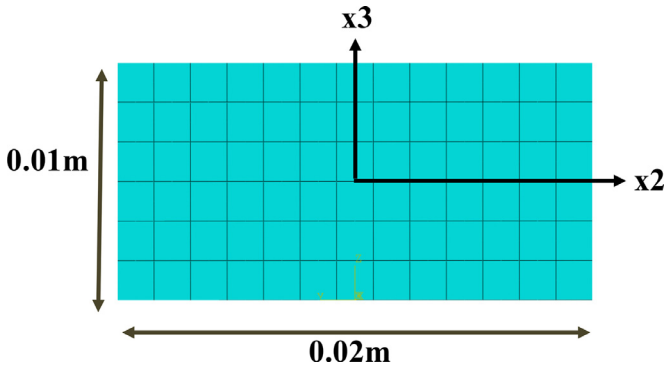

Fig. 5. Schematic of the cross section of single layer piezo-sensor.

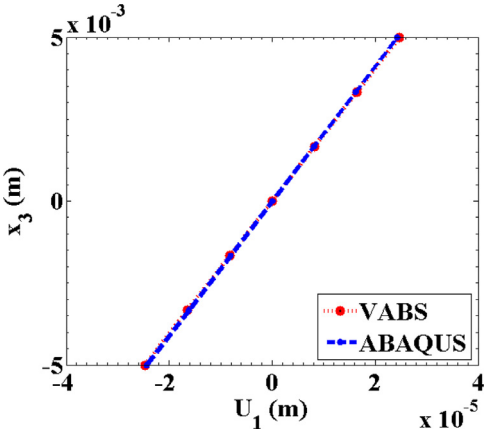

Fig. 6. Displacement in x_1 direction.

Example 8.1. Single layer sensor model under static load

The first example in the process of validation is a 0.1 m long cantilever sensor composed of PZT4 as depicted in Fig. 4. The model is of rectangular cross-section with a width of 0.02 m and thickness of 0.01 m. The material properties are listed in Table 1. The bottom surface is grounded. A constant load of 50 N is applied at the free end.

The 3D ABAQUS sensor model is meshed with 8-noded linear piezoelectric brick elements. The complete structure is composed of 100 elements along the length, 13 elements along the width and 6 elements along the thickness as shown in the Fig. 5. To verify the efficacy of the model we compare the mechanical variables and most importantly electric potential output recovered at the mid span i.e at $x_1 = 0.05$ m obtained from VABS and with 3D ABAQUS simulation. Fig. 6, shows the comparison between the 3D displacement components. The major displacement is along the x_3 direction. The model is capable of capturing the axial, bending in two direction and torsion mode which enhances the flexibility

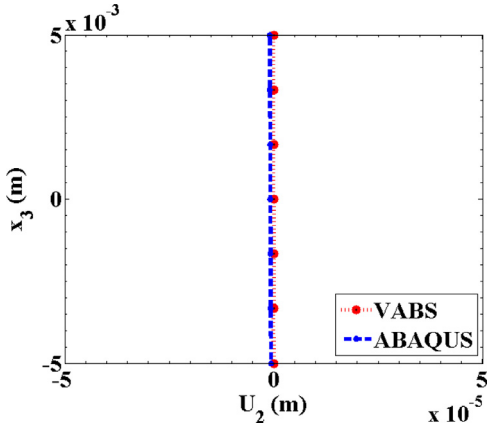

Fig. 7. Displacement in x_2 direction.

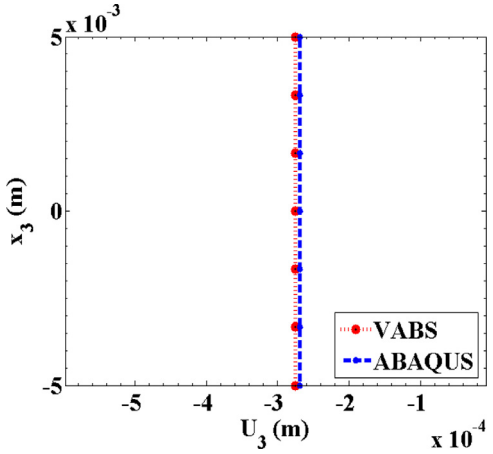

Fig. 8. Displacement in x_3 direction.

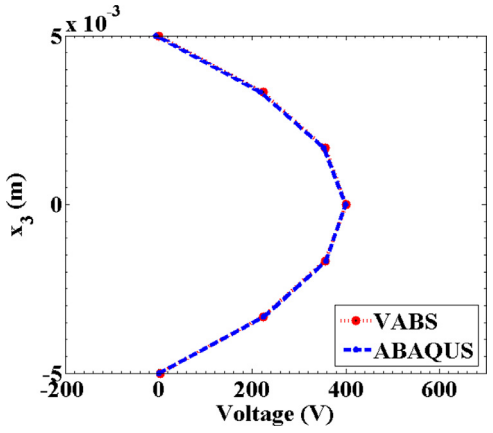

Fig. 9. Voltage distribution across thickness.

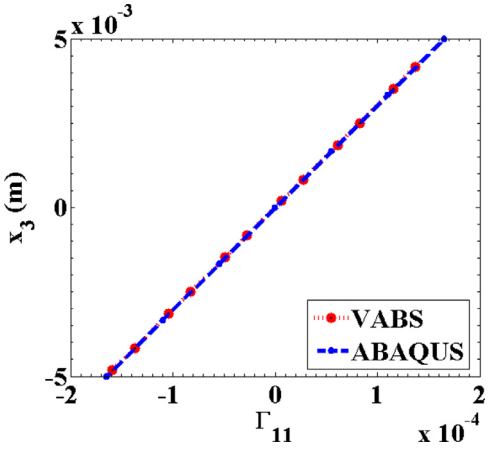

Fig. 10. Strain distribution in x_1 direction.

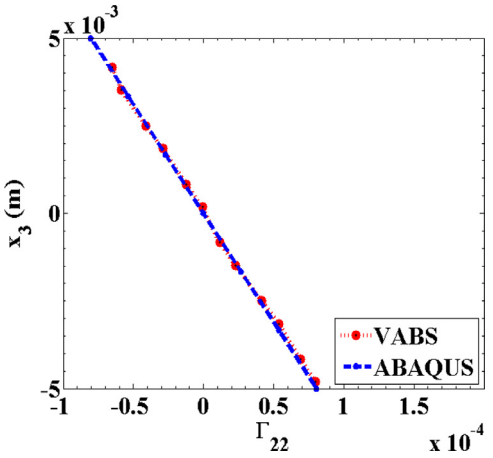

Fig. 11. Strain distribution in x_2 direction.

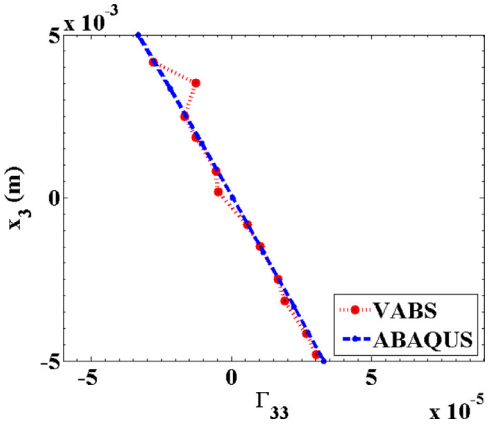

Fig. 12. Strain distribution in x_3 direction.

of the model. The recovered displacement, non zero strain, major stress component and electric potential output as shown in Figs. 6–13, an excellent match with the 3D simulation results. Thus we can depict that the methodology is well capable of generating 3D results with high level of accuracy and at a lower computational cost and time.

Example 8.2. Double layer sensor model under static load

In the second example, we investigate a double layer sensor model comprising of PZT layer bonded with aluminium layer. The model is 0.1 m in length and each layer is of width 0.02 m and thickness 0.005 m. A load of 50 N is applied at its free end. A clear schematic of the model is shown in Fig. 14. Both the layers has been assumed to be perfectly bonded.The interface is grounded. To validate our mathematical result we have performed a 3D simulation with double layer configuration in ABAQUS. A 8-noded quadratic brick element is used to model the aluminum layer and a 8-noded quadratic piezoelectric brick element is used to model the piezoelectric layer. A tie constraint has been applied to ensure perfectly bonded condition in the interface.

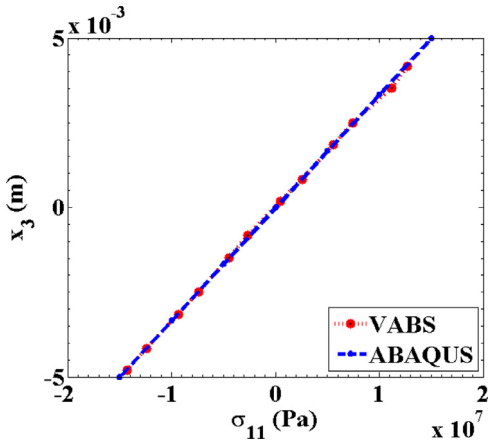

Fig. 13. Stress distribution in x_1 direction.

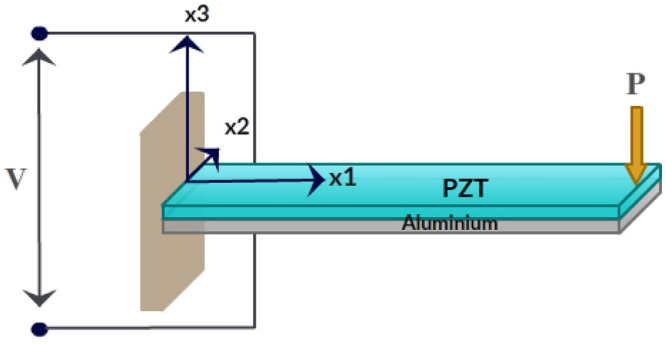

Fig. 14. Double layer piezo-sensor.

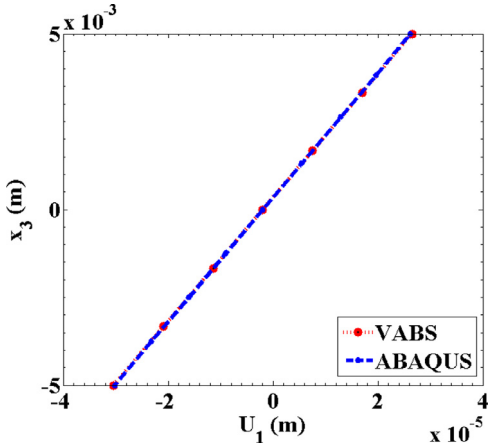

Fig. 15. Displacement in x_1 direction.

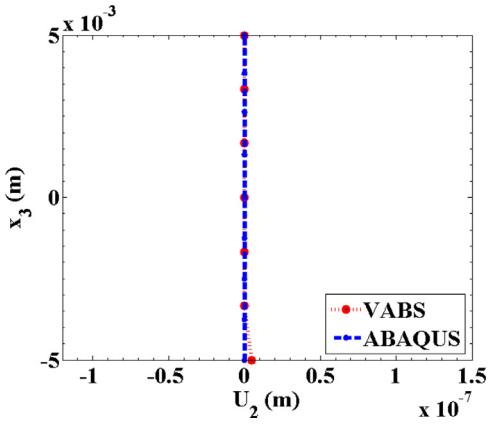

Fig. 16. Displacement in x_2 direction.

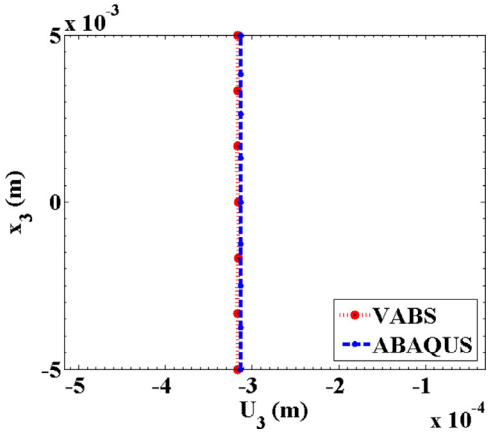

Fig. 17. Displacement in x_3 direction.

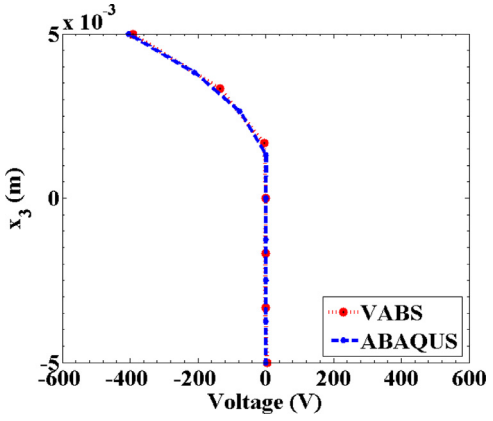

Fig. 18. Voltage distribution.

The accuracy of the reduced order models can be measured on how well it predicts the 3D mechanical as well as electrical variables. Therefore to complete the modeling, recovery relations are needed which we have discussed in the formulation section. Recovery relations means expressing the 3D displacements, stresses, strains, electric potential in terms of 1D beam variables and local cross-sectional coordinates. Fig. 15, shows the recovered 3D displacement in the x_1 direction. Since we have considered Euler–Bernoulli beam theory so the variation of U_1 along its thickness will be linear. U_2 displacement as shown in Fig. 16 is smallest as compared to the other two displacement components. The electric potential across the thickness is recovered through VABS and compared with ABAQUS result as shown in Fig. 18. We can observe that there is a constant 0 V in the aluminium layer which is because there will not be any voltage variation in a passive material. In the piezoelectric layer we get a variation of voltage from 0 V to −400 V. Similarly we plot the 3D strains Γ_{11}, Γ_{22} and Γ_{33} along the thickness direction i.e x_3 direction as shown in Figs. 19–21. The major stress component is shown in Fig. 22. All the recovered results shows a good match proving the accuracy of our methodology for a double layer sensor model as well (Figs. 17 and 23).

Example 8.3. Dynamic analysis of single layer piezo-sensor

There are many sources of mechanical energies which occur in the environment with various frequencies. To capture efficiently

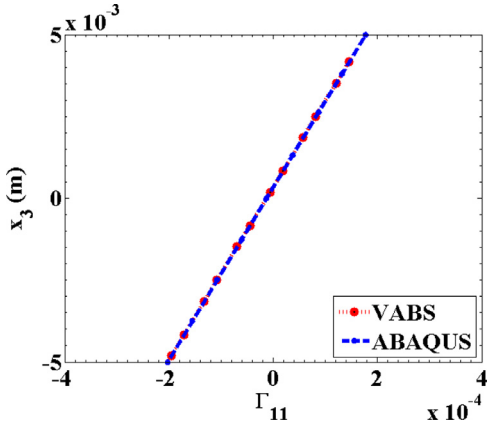

Fig. 19. Strain distribution in x_1 direction.

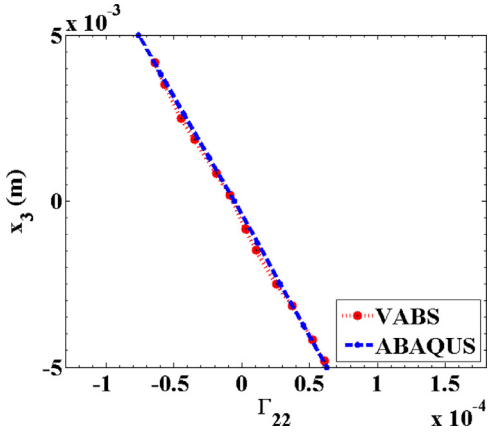

Fig. 20. Strain distribution in x_2 direction.

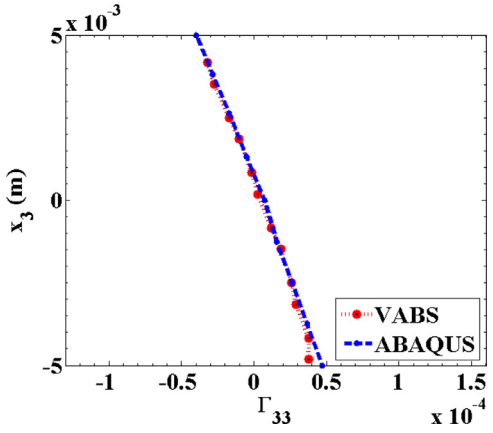

Fig. 21. Strain distribution in x_3 direction.

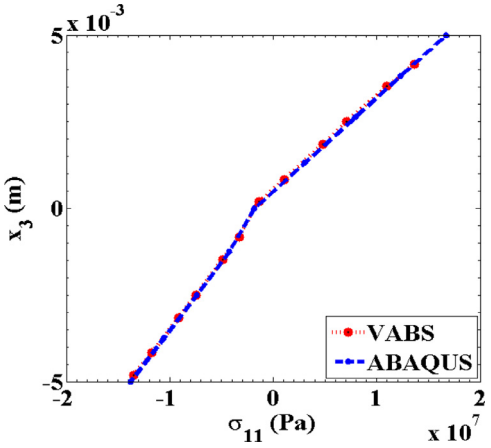

Fig. 22. Stress distribution in x_1 direction.

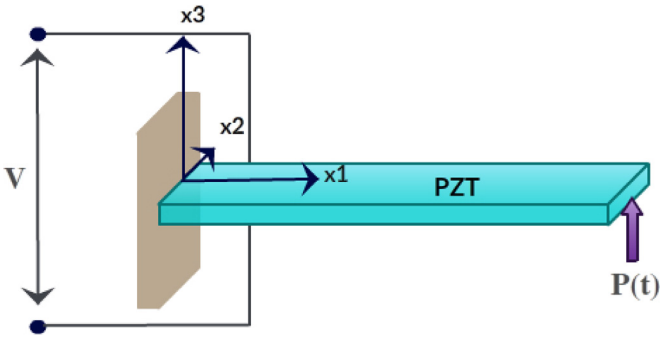

Fig. 23. Single layer piezo-sensor under dynamic load.

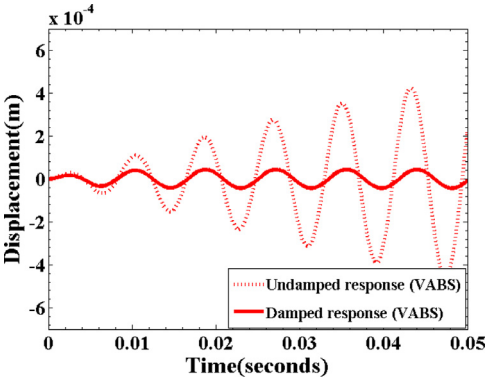

Fig. 24. Displacement response in damped and undamped condition.

the mechanical energies so as to convert it into electrical energies, the eigen frequencies of a piezoelectric cantilever have to operate close to the frequency of the mechanical source. So an efficient mathematical model is needed to define the eigenfrequencies which can be controlled by dimensions of the model and piezoelectric material parameters. As a continuation of the previous validation process, this section tries to develop a single layer mathematical model based on Variational asymptotic method under a time varying load. The eigen frequency for the first mode is 123 Hz and for the second mode is 775 Hz. PZT5H is used to model the single layer sensor. The proposed sensor model provides a full input-output description that can predict the response in both time domain as well as in the frequency domain. The bending stiffness obtained from VABS have been used as an input for the dynamic analysis. The sensor model has been excited at a frequency nearby to its first natural frequency. The forcing function used at the free end node is $F = F_0 \cos(\omega t)$. Here $F_0 = 0.01$ N, ω is the excitation frequency and taken to be 119 Hz which is nearby to its first natural frequency. The model has been studied for a time period of 0.05 s and with a time step of $1e^{-8}$. Central difference scheme method has been used for time integration. The model is studied for both undamped and damped condition. We can see in Fig. 24 the time domain displacement plot of the mid node of the model with and without damping. The damping considered in the model is proportional damping and the system damping matrix

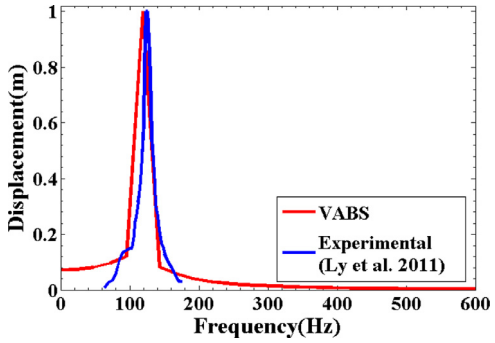

Fig. 25. First mode displacement versus frequency.

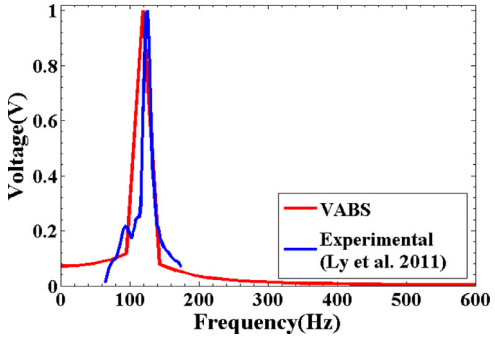

Fig. 26. First mode voltage versus frequency.

can be written as,

$$[C] = \alpha[M_{sys}] + \beta[K_{sys}] \tag{46}$$

where α and β are constants and M_{sys}, K_{sys} are the system mass and stiffness matrix. Proportional damping has an advantage of having same characteristics as the mass or stiffness matrix. The time domain displacement response has been further converted into frequency domain response as shown in Fig. 25 and validated with the experimental work performed by Ly et al. (2011). Similarly Fig. 26 projects the voltage response in frequency domain for the same excitation frequency. The frequency peak clearly corresponds to 119 Hz through VABS and 124 Hz as mentioned in the experimental work by Ly et al. In both the frequency domain response the percentage deviation is around 4 percent, which is negligibly small. One of the reason for the minor deviation can be because of the damping parameters.

9. Conclusions

This paper applies VAM to mathematically develop and analyze a sensor model under static and dynamic load. The detailed description of the theory applied to sensor model has been presented, clearly describing the steps leading to the constitutive model for a sensor, recovery of the field variables as well as the frequency response. The model developed using variational asymptotic method shows a good agreement with the 3D ABAOUS results as well as with experimental result obtained by Ly et al. (2011). The voltage response under a static load shows a constant zero voltage for the passive layer and variation in the PZT layer. Under dynamic load we can clearly see a peak corresponding to the excitation frequency which is nearby to system's first natural frequency for both displacement and voltage response. This whole study is based on the theory of variational asymptotic method which is unlike most theories that prevail on priori assumptions. From this study, we can conclude that the method is very efficient, and can be used to model and analyze any type of sensor with a very high level of accuracy comparable to any standard 3D finite element analysis at a much lower computation time and expense. The present theory is capable of handling sensor model with arbitrary cross section, material, geometry, embedded and surface mounted under any working condition and at a very efficient time process. The general nature of the mathematical theory ensures that it can tackle single layer, multi layer active inclusion, curved as well as prismatic sensor geometry.

Acknowlegment

The authors of this paper would like to thank Prof. Wenbin Yu of Purdue University and his research group 'Composite Design and Manufacturing Hub' for their valuable suggestions in clearing some of our doubts during this research work. The second author acknowledges the funding from Aeronautical Research & Development Board of India, through Grant DARO/08/1031716/M/1 DT 23/1/2014. We are also thankful to the Ministry of Human Resource Development (MHRD), India for their fellowship to the first author and Department of Applied Mechanics-IIT Delhi for their encouragement and help.

References

Abaqus/CAE 6.10, Dassault system 2010.
Abreu Gustavo, L.C.M., Ribeiro, J.F., Steffen, V., 2003. Experiments on optimal vibration control of a fexible beam containing piezoelectric sensors and actuators. Shock Vib. 10, 283–300.
Ali, R., Mahapatra, D.R., Gopalakrishnan, S., 2004. An analytical model of constrained piezoelectric thin film sensors. Sens. Actuators A 116, 424–437.
Ajitsaria, J., Choe, S.Y., Shen, D., Kim, D.J., 2007. Modeling and analysis of a biomorph piezoelectric cantilever beam for voltage generation. Smart Mater. Struct. 16, 447–454.
Berdichevsky, V.L., 1979. Variational asymptotic method of constructing a theory of shells. PMM 43, 664–687.
Buxi, D., Redoute, J.M., Yuce, M.R., 2014. Frequency sensing of medical signals using low voltage piezoelectric sensors. Sens. Actuators A 220, 373–381.
Cesnik, C.E.S., Hodges, D.H., 1997. VABS: a new concept for composite rotor blade cross-sectional modeling. J. Am. Helicopter Soc. 42, 27–38.
Chee, C.Y.K., Tong, L., Steven, G.P., 2006. A review on the modeling of piezoelectric sensors and actuators incorporated in intelligent structures. J. Intell. Mater. Syst. Struct. 9, 3–19.
Dalessandro, L., Rosato, D., 2005. Finite-element analysis of the frequency response of a metallic cantilever coupled with a piezoelectric transducer. IEEE Trans. Instrum. Meas. 54, 1881–1890.
Hodges, D.H., 2006. Nonlinear Composite Beam Theory. AIAA, Washington, DC.
Han, H., Kim, J., 2013. Active muscle stiffness sensor based on piezoelectric resonance for muscle contraction estimation. Sens. Actuators A 194, 212–219.
Kursu, O., Kruusing, A., Pudas, M., Rahkonen, T., 2009. Piezoelectric bimorph charge mode force sensor. Sens. Actuators A 153, 42–49.
Kapuria, S., Yasin, M.Y., 2010. Active vibration control of piezoelectric laminated beams with electrode actuators and sensors using an efficient finite element involving an electric node. Smart Mater. Struct. 19, 045019.
Kapuria, S., Yasin, M.Y., 2013. Active vibration control of smart plates using directional actuation and sensing capability of piezoelectric composites. Acta Mech. 224, 1185–1199.
Kalantarian, H., Alshurafa, N., Le, T., Sarrafzadeh, M., 2015. Monitoring eating habits using a piezoelectric sensor-based necklace. Comput. Biol. Med. 58, 46–55.
Ly, R., Rguiti, M., Astorg, S.D., Hajjaji, A., Courtois, C., Lerichea, A., 2011. Modeling and characterization of piezoelectric cantilever bending sensor for energy harvesting. Sens. Actuators A 168, 95–100.
Ng, T.H., Liao, W.H., 2005. Sensitivity analysis and energy harvesting for a self powered piezoelectric sensors. J. Intell. Mater. Syst. Struct. 16, 785–797.
Neto, M.A., Yu, W., Roy, S., 2009. Two finite elements for general composite beams with piezoelectric actuators and sensors. Finite Elements Anal. Des. 45, 295–304.
Olszewski, O.Z., Houlihan, R., Keeffe, R.O'., Neill, M.O'., Waldron, F., Mathewson, A., Jackson, N., 2014. A MEMS silicon-based piezoelectric AC current sensor. Procedia Eng. 87, 1457–1460.
Payo, I., Hale, J.M., 2011. Sensitivity analysis of piezoelectric paint sensors made up of PZT ceramic powder and water based acrylic polymer. Sens. Actuators A 168, 77–89.
Roy, S., Yu, W., 2009. Dimensional reduction of a piezoelectric composite rod. European Journal of Mechanics A/Solids28, 368–376.
Roy, S., Yu, W., Han, D., 2007. An asymptotically correct classical model for smart beams. Int. J. Solids Struct. 44, 8424–8439.
Roy, S., Yu, W., 2009. Dimensional reduction of a piezoelectric composite rod. Eur. J. Mech. A/Solids 28, 368–376.
Shen, M.H.H., 1994. Analysis of beams containingpiezoelectric sensors and actuators. Smart Mater. Struct. 3, 439–447.

Sodano, H.A., Inman, D.J., 2005. Comparison of piezoelectric energy harvesting devices for recharging batteries. J. Intell. Mater. Syst. Struct. 16 (10), 799–807.
Williams, C.B., Yates, R.B., 1996. Analysis of a micro-electric generator for microsystems. Sens. Actuators A 52, 8–11.
Wang, Q., Quek, S.T., 2002. A model for the analysis of beams with embedded piezoelectric layers. J. Intell. Mater. Syst. Struct. 13, 61–70.
Wang, S.Y., 2004. A finite element model for the static and dynamic analysis of piezoelectric bimorph. Int. J. Solids Struct. 41, 4075–4096.
Yang, S.M., Lee, Y.J., 1994. Interaction of structure vibration and piezoelectric actuation. Smart Mater. Struct. 3, 494–500.
Yu, W., 2002. Variational asymptotic modeling of composite dimensionally reducible structures, (PhD. thesis), Georgia Institute of Technology.
Yu, W., Hodges, D.H., 2004. Elasticity solutions versus asymptotic sectional analysis of homogeneous, isotropic, prismatic beams. J. Appl. Mech. 71, 15–23.
Yu, W., 2011. VABS Manual for Users.
Yu, W., Hodges, D.H., Ho, J.C., 2012. Variational asymptotic beam sectional analysis – an updated version. Int. J. Eng. Sci. 59, 40–64.
Zhou, W., Khaliq, A., Tang, Y., Ji, H., Selmic, R.R., 2005. Simulation and design of piezoelectric microcantilever chemical sensors. Sens. Actuators A 125, 69–75.
Zhoua, L., Sun, J., Zheng, X.J., Denga, S.F., Zhao, J.H., Peng, S.T., Zhang, Y., Wang, X.Y., Cheng, H.B., 2012. A model for the energy harvesting performance of shear mode piezoelectric cantilever. Sens. Actuators A 179, 185–192.